Titan IIIC Preflight and Postflight Trajectory Analyses

Prabhakara P. Rao*
Martin Marietta Corporation, Denver, Colorado

The Titan IIIC launch vehicle uses a carousel inertial measurement unit to provide acceleration and attitude information during its flight to geosynchronous orbit. The four-gimbal inertial measurement unit imposes certain middle gimbal angle constraint on trajectory design. To meet this constraint, various maneuver times and vehicle orientations are optimized during engineering trade studies. The preflight trajectory analysis ensures that all mission specifications, trajectory requirements, and instrument constraints are satisfied for a particular Titan IIIC launch vehicle and spacecraft combination. In-flight recording of guidance, navigation, and performance variables in a telemetry stream enables postflight reconstruction of an instrument-sensed trajectory. An independent trajectory reconstruction is achieved by using the recursive Kalman minimum variance filtering algorithms to fit the equations of motion to radar tracking data. A comparison between the preflight, instrument-sensed, and postflight reconstructed trajectories, together with orbital error bounds determined by a statistical error analysis, provides the mission accuracy. The purpose of this paper is to provide an overview of the preflight, postflight, and accuracy analyses of the Titan IIIC launch vehicle.

Introduction

SUCCESS of a space mission is measured by the accuracy with which the payload is injected into its final orbit. The payload is usually capable of correcting small injection errors[1] and performing small maneuvers to attain a desired orbit. To a large extent, the final orbit accuracy depends on the actual trajectory of a launch vehicle with respect to the preflight predicted trajectory. Although the preflight trajectory could be determined accurately with extensive mathematical models and simulations, determining the postflight trajectory is limited by the availability of telemetered instrument-sensed data or radar tracking data. Therefore, the postflight trajectory reconstruction plays an important role in determining payload injection accuracy. Furthermore, the postflight analysis provides useful information about the characteristics of measuring instruments subjected to a flight environment. The error analysis based on a nominal preflight trajectory will determine the bounds on injection errors due to noncompensable or unpredictable instrument errors. The purpose of this paper is to provide an overview of the preflight, postflight, and accuracy analyses of the Titan IIIC launch vehicle that injects payloads into geosynchronous orbits. This requires a basic understanding of the launch vehicle, mission sequence, and acceleration and attitude-sensing instruments.

Vehicle Description

The Titan IIIC vehicle has an overall height of 108 ft and is a four-stage space launch vehicle: Stages 0-III. Stage 0 consists of two solid rocket motors that are strapped to opposite sides of Stages I and II. These motors furnish the initial boost power for the Titan IIIC flights and have a nominal burn time of 106-108 s for typical geostationary missions. Thrust vector control during Stage 0 flight is provided by the secondary injection of liquid nitrogen tetroxide (N_2O_4) into a fixed nozzle. Stages I and II both use liquid propellants. The rocket engines for both core stages are hydraulically gimbaled and fed by turbopumps. A heat shield and engine exit nozzle closures protect Stage I engines from thermal radiation and exhaust gas recirculation during Stage 0 flight.

Stage III (transtage) consists of control and propulsion modules. The control module contains flight control, attitude control, guidance, and other avionic equipment, while the propulsion module contains the liquid propulsion system for the main engines. Attitude control for the vehicle is provided by six rocket engine modules that each contain two individual thrusters. These are fired intermittently to provide control moments about the transtage pitch, yaw, and roll axes, and to maintain proper attitudes during thermal control, telemetry, and spacecraft separation maneuvers.

Mission Description

A typical mission begins with Stage 0 solid rocket motor (SRM) ignition and liftoff. After clearing the launch pad, the launch vehicle rolls to a desired flight azimuth and begins to pitch over in the plane of trajectory. At approximately 110 s after liftoff, the inertial guidance system senses a decreasing acceleration level and the Stage I engines are ignited when acceleration falls below $2g$. Twelve seconds later the solid rocket motors are jettisoned. As Stage I propellant is depleted, the thrust chamber pressure switch (TCPS) shuts down Stage I engines and sends a signal to ignite the Stage II engine and to fire explosive mating bolts to separate the core stages. The payload fairing is nominally jettisoned at 305 s after liftoff at an altitude where aerodynamic effects are negligible. Sixteen seconds after Stage II shutdown, the Stage II retrorockets are ignited to separate the transtage from Stage II. For a typical synchronous equatorial mission, the transtage engine is fired at either the first or second equatorial crossing for approximately 315 s to effect the elliptical transfer to synchronous altitude. After a 5-h coast period, during which the transtage performs thermal and telemetry orientation maneuvers, the transtage and spacecraft arrive at synchronous altitude (19,323 n.mi.). During the transfer orbit flight, the transtage is oriented to point the roll axis along an inertially fixed direction and commanded a continuous roll for spacecraft thermal control. At the end of transfer orbit coast, the transtage engine is restarted for approximately 110 s to circularize the orbit and reduce the orbital inclination to a desired value. The transtage is oriented to payload separation attitude and, at a specified time from final orbit inject, the spacecraft is separated. A typical mission sequence of events is presented in Table 1, and orbits and their mercator projections are shown in Fig. 1.

Presented as Paper 81-2426 at the AIAA/SETP/SFTE/SAE 1st Flight Testing Conference, Las Vegas, Nev., Nov. 11-13, 1981; submitted Nov. 24, 1981; revision received Jan. 3, 1983.

*Group Engineer, Titan 34D/Transtage Guidance Analysis and Validation. Member AIAA.

Instrument Description

The Carousel VB inertial measurement unit (IMU) used in the Titan IIIC vehicle is a four-gimbal, all-attitude inertial platform stabilized by three, single-degree-of-freedom, gas-bearing, rate-integrating gyros. The lower portion of the platform, on which the x and y gyros and accelerometers are mounted, is rotated at 1 rpm about an inertially fixed axis. The other set of gyros and accelerometers is mounted on a turret, the nonrotating element of the system. Figure 2 illustrates the Carouseled VB gimbal and platform configuration and its mounting within the Titan IIIC vehicle. With this configuration, accelerometer bias and gyro fixed-torque drift of the carousel instruments become sinusoidally modulated in inertial space. This obviates the growth of noncompensable errors in these parameters in the carousel plane. The IMU transmits acceleration and gimbal angle data to the missile guidance computer (MGC) for guidance and navigation calculations. The gimbal angles are measured with synchros and resolvers.

Preflight Trajectory Analysis

Preflight activities include: a three-degree-of-freedom guidance reference trajectory analysis and a six-degree-of-freedom pretest trajectory analysis. The guidance reference trajectory is an open-loop guidance and control system point-mass analysis that incorporates specific performance characteristics for the particular Titan IIIC launch vehicle. It is an optimized trajectory designed to meet all mission specifications and trajectory constraints, such as maximum dynamic pressure, aerodynamic heating rate, and staging constraints. The results of this analysis are used primarily to provide a basis for generating final guidance system parameters and updating baseline mission performance.

The six-degree-of-freedom pretest trajectory incorporates closed-loop guidance steering and control system stabilization. This final pretest trajectory provides: 1) prelaunch vehicle performance, 2) final inputs to range safety, 3) information for tracking operations, 4) scientific verification of guidance system parameters, 5) a nominal trajectory for error analysis, and 6) a basis for postflight analysis.

In addition to performance evaluation during preflight activities, a six-degree-of-freedom trajectory can be used to determine the variation of platform gimbal angles during the entire mission. The outer gimbal angle γ, and inner gimbal angle α can traverse from 0 to 360 deg, whereas the middle gimbal angle β is restricted to travel from only -90 to $+90$ deg. To avoid gimbal flip in an actual flight the beta gimbal angle traverse is restricted to between -80 and $+80$ deg with a ± 10-deg margin to account for any uncertainty in pad alignment, autopilot limit cycle, autopilot overshoot, time, and IMU dispersions.

Several approaches are used during mission planning stages to prevent the beta gimbal angle from exceeding the ± 80-deg limit. One approach, which could be used during transfer orbit maneuvers to transmit telemetry signals to ground stations, is to search for an initial pitch-axis direction. This approach is suitable for missions in which the roll axis is pointed toward an inertially fixed direction to meet the transfer orbit thermal requirements of a payload. During the transfer orbit, periodic deviations from the thermal orientation will be necessary to permit reception of transtage telemetry signals. These telemetry orientations or "dipouts" will point the telemetry antenna Earthward either at the geocenter or at a specified ground station. At the end of dipout interval, the transtage will perform a thermal orientation maneuver followed by a continuous roll for spacecraft thermal control. Figure 3 illustrates the variation in the maximum beta gimbal angle for various dipout maneuvers as the pitch axis is rotated from 0 to 360 deg from an initial direction. The figure shows that certain pitch-axis directions as specified by the roll angle in the shaded interval can be selected to meet the ± 80-deg beta gimbal angle constraint during engineering trade studies to optimize the dipout maneuvers. This approach is suitable when the initial and final attitudes for the maneuver are independent of (or weakly dependent on) vehicle performance.

When the vehicle attitude maneuver depends strongly on vehicle performance, the beta gimbal constraint can be satisfied by finding either the initial start attitude or an intermediate attitude. Because the second burn orientation time is a performance-dependent event, the initial attitude of the vehicle from which the reorientation maneuver takes place could be restricted so that the pitch axis is outside a gimbal flip avoidance sector. The guidance parameters, which define the flight-plan-dependent gimbal flip sector, are determined by analysis during the planning stages. If the pitch axis orientation falls within the sector, the thermal roll is con-

Table 1 Titan IIIC typical mission sequence of events

Event	Time from ignition, s
SRM ignition	0
Begin roll maneuver	6
Terminate roll maneuver	9
First pitch rate	10
Second pitch rate	20
Begin load relief	30
Terminate load relief	80
2g sensed, start Stage I engine	110
SRM jettison	122
Begin closed-loop steering	126
Stage II start, Stages I and II separation	255
Payload fairing jettison	305
Stage II shutdown	462
Stage II jettison, park orbit inject	478
Start transtage first burn	4,119
End transtage first burn	4,434
Start velocity vernier burn	4,534
End velocity vernier burn	4,542
Start transtage second burn	23,317
End transtage second burn	23,427
Payload separation	23,640

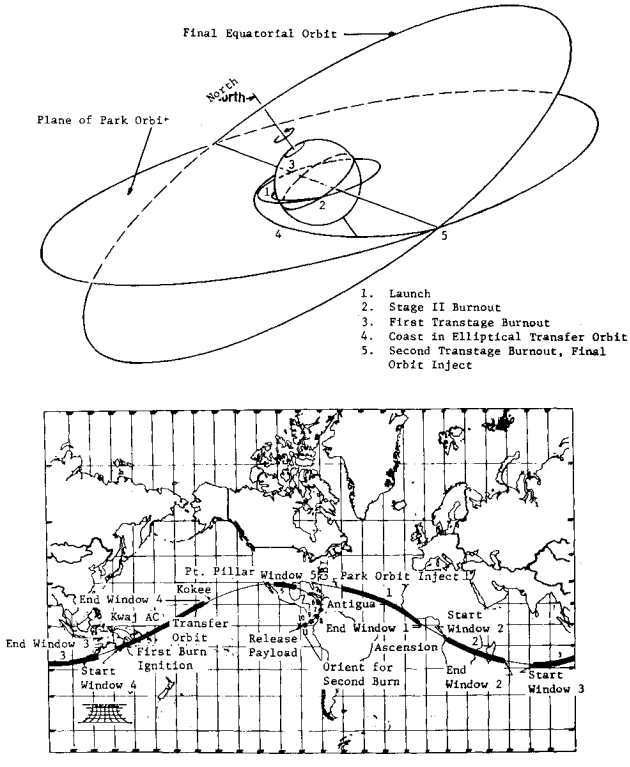

Fig. 1 Mission description.

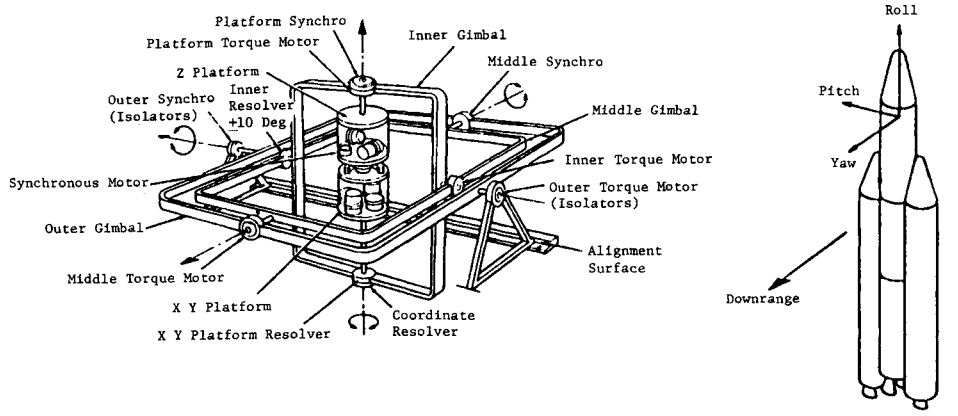

Fig. 2 Titan IIIC Carousel VB inertial measurement unit.

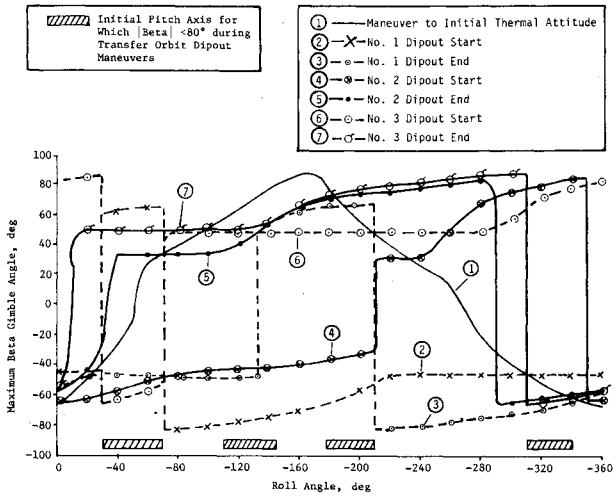

Fig. 3 Effect of initial pitch axis on transfer orbit maneuvers.

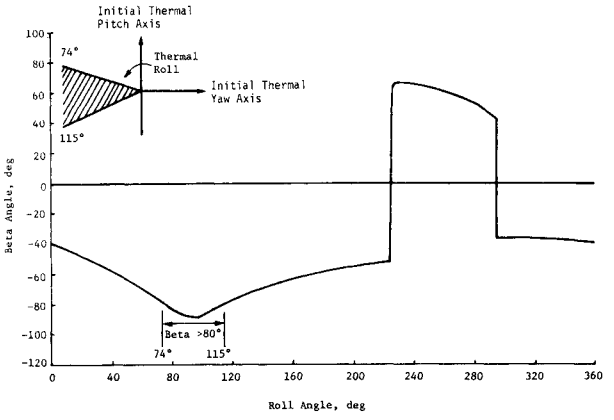

Fig. 4 Variation of beta gimbal angle with roll angle.

tinued to delay the reorientation maneuver. Figure 4 illustrates the variation of beta gimbal angle with roll angle and defines the beta gimbal avoidance sector for a particular mission.

The "intermediate attitude" approach can be used to satisfy the beta gimbal angle constraint when both initial and final maneuvers are well defined. Instead of maneuvering directly to a final attitude, the vehicle is maneuvered from the initial attitude to an intermediate attitude and then to the final attitude. During this maneuver the beta gimbal angle traverse can be restricted to lie within the ±80-deg sector. A universal

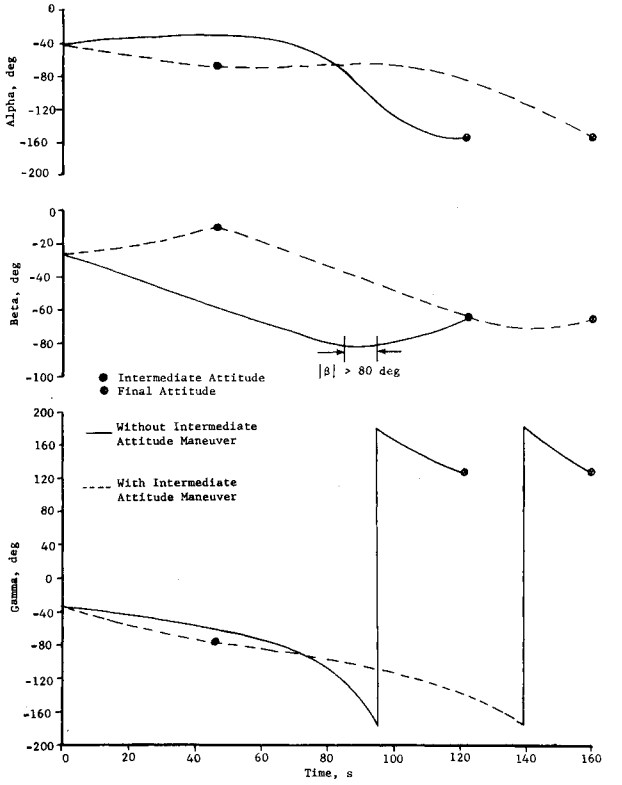

Fig. 5 Variation of α, β, γ, during a maneuver.

intermediate attitude direction can be determined to account for performance dispersions. Figure 5 shows the variations of the α, β, and γ angles with and without the intermediate maneuver. Although the beta gimbal angle is constrained, the propellant required and the time to complete the maneuver are slightly increased.

Postflight Trajectory Reconstruction

The postflight analysis for the Titan IIIC vehicle is carried out for the entire flight from liftoff to the end of the mission. During powered flight phases of the mission and dipout intervals during coast, the vehicle orients to transmit telemetry data to ground stations. Also, the vehicle is tracked using radar to provide an independent verification of the trajectory. Both telemetry and radar data are analyzed to determine the mission accuracy.[2]

Telemetry Data Reduction

Atmospheric Flight

The performance of the Titan IIIC vehicle as it passes through the atmosphere during the first 200 s of flight is

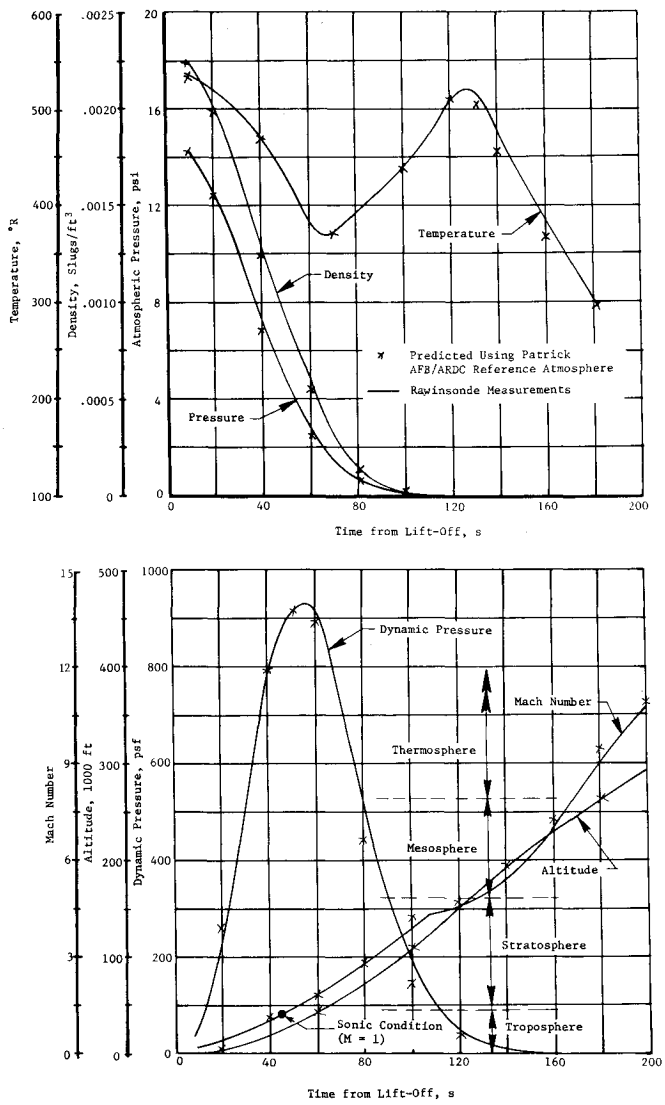

Fig. 6 Atmospheric flight characteristics.

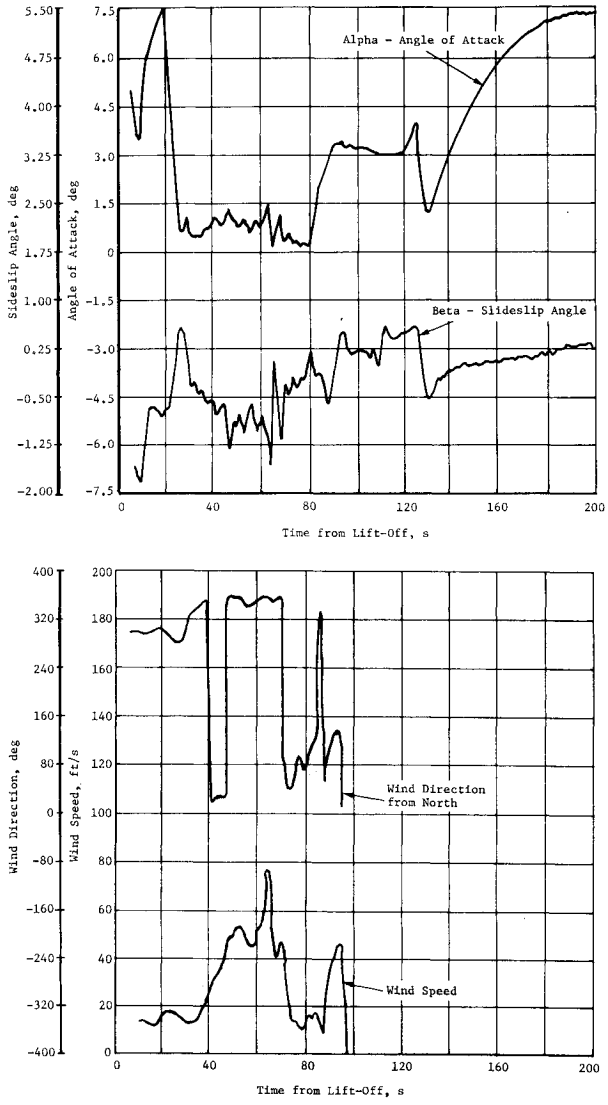

Fig. 7 Atmospheric wind characteristics.

analyzed using time zero (T-0) Rawinsonde balloon sounding measurements of atmospheric parameters to an altitude of 101,000 ft, and Patrick reference atmosphere beyond that altitude. These measurements provide meteorological data, such as atmospheric pressure, density, temperature, wind speed, and wind direction in the vicinity of Air Force Eastern Test Range (AFETR) pad 40 at the time of launch. These data are depicted in Figs. 6 and 7 along with those predicted using AFB/ARDC reference atmosphere. The vehicle reaches tropopause, stratopause, and mesopause in about 60, 125, and 180 s, respectively. Figure 6 also shows the variation of Mach number, which shows that the vehicle acceleration is reduced slightly at the time of separation of Stages 0 and I, and also that the vehicle attains supersonic speed at an altitude of about 18,670 ft. Different open-loop pitch rates at 10, 20, 30, and 80 s, and yaw steering between 15 and 109 s, produce significant variation in the angle of attack and angle of sideslip (Fig. 7). Both the angle of attack and sideslip angle are relatively small in the interval between 30 and 80 s assisting in the reduction of aerodynamic load on the vehicle. The aerodynamic loads in the pitch and yaw directions are proportional to the product of dynamic pressure and angle of attack and sideslip angle, respectively. The pitch polynomial and yaw steering are designed to produce aerodynamic load relief between 30 and 80 s. The aerodynamic heating rate, which is proportional to the product of dynamic pressure and vehicle speed relative to wind, and the heating indicator, which represents the accumulation of heat over a period since liftoff, are within constraint values.

Powered Flight

The Titan IIIC launch vehicle, which consists of two solid rocket motors for Stage 0, and three liquid propulsion systems for Stages I, II, and III, injects a payload into a synchronous orbit. The powered flight durations for Stages 0, I, II, and Stage III first and second burns are approximately 109, 145, 210, 315, and 110 s, respectively. The accelerations imparted to the vehicle due to propulsion thrust at various stages of burn are measured by a set of three accelerometers in the IMU. After compensating for accelerometer bias, scale factor, nonlinearities, and misalignments, the summation of accelerometer counts over each minor cycle (0.04 s) in three platform directions are transformed into the vehicle body coordinate frame. The body accelerations during various powered flight phases are plotted on a minor cycle basis in Fig. 8. These show large fluctuations of body acceleration in the transonic flow region for approximately 30-50 s. This phenomenon is attributed to shock waves on the surface and in front of the vehicle when the external flow approaches the sonic condition. In addition to various in-flight transients, the figure clearly shows the transition between thrust decay of Stage 0 and thrust buildup of Stage I and the propellant settling burns of the attitude control system (ACS) before transtage first and second burns in low gravitational fields. In

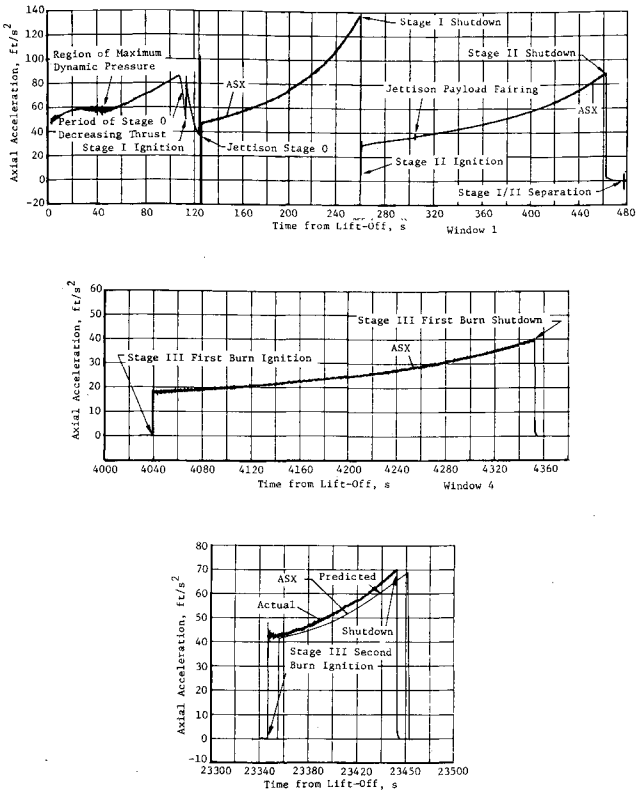

Fig. 8 Axial thrust acceleration variation.

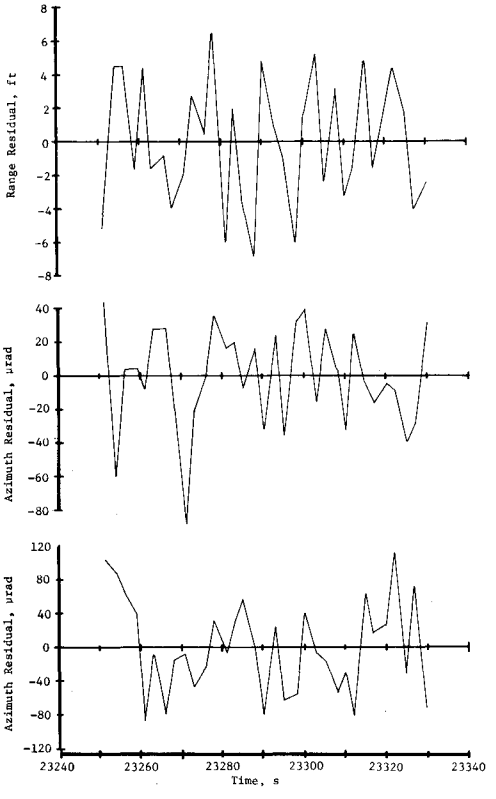

Fig. 10 Variation of residuals between computed and measured data.

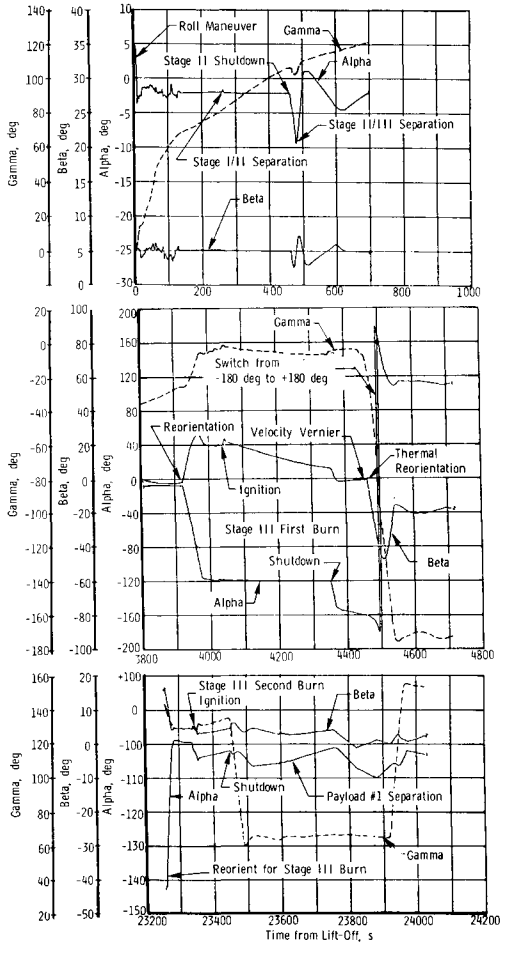

Fig. 9 Variation of α, β, γ during boost, transtage first and second burns.

Fig. 8, a time dispersion at transtage second burn ignition is due to initiation of the burn based on a specified vehicle distance from the desired final orbit plane instead of a time from liftoff.

Coast Flight

During the coast flight phase of the Titan IIIC vehicle, the ACS imparts small amounts of thrust to provide the necessary thermal and telemetry dipout maneuvers, vehicle reorientation and propellant settling before main engine ignition, and velocity vernier burn to fine-tune the transfer orbit parameters. Because the in-flight accelerometer biases may be different from the factory or prelaunch calibrated values, coasting periods can be used to determine the in-flight variation in bias terms. The accelerometer biases are computed by summing the accelerometer counts over a coasting period in which there is no ACS pulsing. Because the accelerometer biases are sensitive to flight thermal environments, the in-flight calibration of biases normally indicates a Z-bias shift at the end of the boost phase.

Gimbal Angles

The actual attitude of the vehicle during flight is determined from gimbal angles obtained from synchro outputs. In postflight analysis on a major cycle (1 s) basis, the platform inner gimbal angle α, middle gimbal angle β, and outer gimbal angle γ, are calculated from the sine and cosine of these angles. Because the inner gamma gimbal angle has very limited travel (± 10 deg), only the sine of this angle is telemetered on every major cycle. Figure 9 shows the variation of α, β, and γ during the boost phase and near the transtage first and second burns.

Radar Data Reduction

An independent and simple method of verifying the trajectory of a launch vehicle is by determining the orbit using radar tracking data. The vehicle trajectory during the powered flight portion of the mission can be reconstructed by

Table 2 Inertial measurement unit class error budget

Error class	Error source	1σ error value
Accelerometer	Scale factor *x, y, z*	70.2 ppm[a]
	Bias *x, y*	86.7 μg
	Bias *z*	30.44 μg
	Nonlinearity *x, y, z*	10.0 $\mu g/g^2$
	Cubic term *x, y, z*	0.5 $\mu g/g^3$
	Misalignment *x-y*	25 arc-s
	Misalignment *x-y, y-z*	13 arc-s
	Misalignment *z-x, z-y*	10 arc-s
Gyro	Drift *x, y*	8 meru[b]
	Drift *z*	2.15 meru
	Input axes mass unbalance *x, y, z*	5.0 meru/g
	Spin axes mass unbalance *x, y*	8.0 meru/g
	Spin axes mass unbalance *z*	3.64 meru/g
	Output axes mass unbalance *z*	3.0 meru/g
	Major compliance *x, y, z*	1.7 $meru/g^2$
Turret	Misalignment	5.0 arc-s
Platform	Misalignment *x, y*	20 arc-s
	Misalignment *z*	65 arc-s

[a] Parts per million. [b] Milli-Earch-rate units (0.015 deg/h).

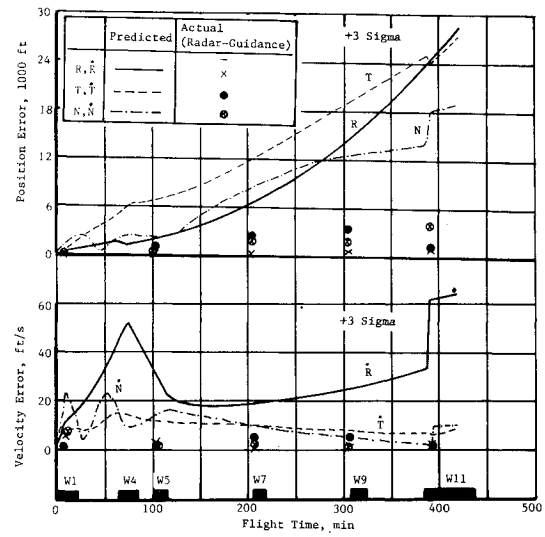

Fig. 11 Variation of mission accuracy.

integrating the equations of motion using predicted thrust acceleration and the attitude model or the airborne accelerometer and gyro measurement data. The recursive Kalman minimum-variance filtering algorithms are used to fit these equations of motion to trajectory measurement data. The process becomes considerably simplified during coast periods above the Earth's atmosphere. Reference 3 describes in detail the use of Kalman filters for estimating boost trajectory using radar data and estimating uncertain dynamic model and measurement parameters. In this postflight analysis, the radar measurement data [range (R), azimuth (A) and elevation (E)] from different tracking stations are used to determine park, transfer, and final orbit parameters. Because the initial state vectors for integration of the equations of motion are unknown, an initial estimation could be improved by a smoothing process. After chronologically filtering the measurement data from initial time to final time, a best estimate of the state vector at final time, based on the processing of all the data, is obtained. During the smoothing process, the final state estimate is integrated backward, from final time to initial time, to provide an improved estimation of the initial conditions. The process of forward filtering and backward smoothing is repeated several times until the residual between the measured value and estimated value is negligible. Figure 10 illustrates the variation of residuals in range, azimuth, and elevation angle measurements obtained during final orbit trajectory reconstruction.

Trajectory Accuracy Analysis

The accuracy with which the transtage can be injected into a desired orbit depends on the performance of guidance and navigation systems in the vehicle. Instrument errors in the guidance hardware cause a deviation between the actual and desired orbits. The guidance accuracy can be determined by comparing the telemetered value of vehicle position and velocity with corresponding values obtained from radar tracking, and then comparing these differences with error bounds obtained from the flight-specific error analysis.

The total error at injection resulting from the flight consists of 1) accelerometer and gyro errors, 2) vehicle performance dispersions, 3) initial alignment errors, and 4) flight control uncertainties. A class error budget (Table 2) along with an acceleration profile generated by pretest trajectory analysis is used to compute state variable errors by a linear perturbation method and multivariate Gaussian statistics. The acceleration errors $\vec{\Delta a}$ are generated on a continuous time-history basis as a sum of instrument-sensed errors and gravity feedback errors. The acceleration errors are given by:

$$\vec{\Delta a} = \vec{\Delta A} - \phi \times \vec{a}_s + \vec{a}_g$$

where

$\vec{\Delta A}$ = translation-generated errors
$\phi \times \vec{a}_s$ = acceleration errors generated by attitude drift error sources
$\vec{a}_g$ = gravity feedback errors
$\vec{a}_s$ = sensed acceleration

The total acceleration errors $\vec{\Delta a}$ are integrated using a trapezoidal integration scheme to compute vehicle velocity and position errors represented by a covariance error matrix. The effect of guidance errors on orbital element dispersions is evaluated by using a Monte Carlo approach.[4]

Guidance system accuracy is determined by computing position and velocity differences between radar and telemetry in the radial-tangential-normal frame, and comparing them with the error bounds obtained from a flight-specific error analysis. Figure 11 depicts a typical Titan IIIC launch vehicle accuracy at various phases of the flight that shows the guidance errors are well within the predicted 3σ limit.

Concluding Remarks

An overview of preflight, postflight, and accuracy analyses of the Titan IIIC launch vehicle, which injects payloads into geosynchronous orbits, is presented. To meet various mission specifications, trajectory requirements, and instrument constraints, significant effort should be made during preflight trajectory analysis activities. Gimbal flip avoidance algorithms in the flight software, and considerable beta gimbal analysis ensures a singularity-free trajectory. Postflight trajectory reconstruction with telemetry and radar data provides not only the accuracy of the mission, but also certain insight into better simulations of preflight trajectories for future missions.

References

[1] Rao, P. P., "Monte Carlo Analysis of Impulse Requirements for Injection Error Correction," *Journal of Guidance and Control,* Vol. 1, July-Aug. 1978, pp. 225-231.

[2] "TIIIC-27 Inertial Guidance System Post Flight Report, Volume I," Martin Marietta Corp., Denver, Colo., MCR-74-301, Sept. 1974.

[3] Wagner, W. E. and Serold, A. C., "Statistical Trajectory Estimation Programs, Vol. I: Formulation," NASA CR 1482, Jan. 1970.

[4] "Total System Error Analysis for Flight Plan VIIM," Martin Marietta Corp., Denver, Colo., MCR-79-099, Oct. 1979.